

Analyses of assumptions and errors in the calculation of stomatal conductance from sap flux measurements

BRENT E. EWERS^{1,2} and RAM OREN¹

¹ Nicholas School of Environment, Duke University, Durham, NC 27708-0328, USA

² Present address: University of Wisconsin, Department of Forest Ecology and Management, 120 Russell Laboratories, 1630 Linden Dr., Madison, WI 53706, USA

Received June 4, 1999

Summary We analyzed assumptions and measurement errors in estimating canopy transpiration (E_L) from sap flux (J_S) measured with Granier-type sensors, and in calculating canopy stomatal conductance (G_S) from E_L and vapor pressure deficit (D). The study was performed in 12-year-old *Pinus taeda* L. stands with a wide range in leaf area index (L) and growth rate. No systematic differences in J_S were found between the north and south sides of trees. However, J_S in xylem between 20 and 40 mm from the cambium was 50 and 39% of J_S in the outer 20-mm band of xylem in slow- and fast-growing trees, respectively. Sap flux measured in stems did not lag J_S measured in branches, and time and frequency domain analyses of time series indicated that variability in J_S in stems and branches is mostly explained by variation in D . Therefore, J_S was used to estimate transpiration, after accounting for radial patterns. There was no difference between D and leaf-to-air vapor pressure gradient, and D did not have a vertical profile in stands of either low or high L suggesting a strong canopy–atmosphere coupling. Therefore, D estimated at one point in the canopy can be used to calculate G_S in such stands. Given the uncertainties in J_S , relative humidity, and temperature measurements, to keep errors in G_S estimates to less than 10%, estimates of G_S should be limited to conditions in which $D \geq 0.6$ kPa.

Keywords: air temperature, air vapor pressure deficit, leaf temperature, leaf-to-air vapor pressure deficit, relative humidity, time lags.

Introduction

Stomata respond to environmental variation, regulate water loss and carbon dioxide gain, and thus biosphere–atmosphere exchange of mass and energy. From porometry measurements, leaf conductance (g_s) can be calculated with Fick's law as:

$$g_s = \frac{E_L}{\delta_w}, \quad (1)$$

where E_L is transpiration per unit leaf area ($\text{mol m}^{-2} \text{s}^{-1}$), and δ_w (mol mol^{-1}) is the water vapor pressure gradient between

the substomatal cavity and the air near the leaf surface (Percy et al. 1989). Mean g_s of the canopy ($\langle g_s \rangle$; $\text{mol m}^{-2} \text{s}^{-1}$) (Sellars et al. 1997, Baldocchi and Meyers 1998, Pataki et al. 1998a), can be obtained from measurements of g_s at several levels in the canopy, together with the vertical distribution of leaf area, and models describing stomatal responses to environmental gradients within the canopy (Jarvis 1995). However, variation among porometric measurements of g_s is large (Jarvis 1995, Hinckley et al. 1998). Leverenz et al. (1982) calculated that, in a uniform monospecific Norway spruce canopy, the number of sample leaves needed to produce an estimate within 10% of the mean at each time step may exceed 150 even if sampling is stratified by major sources of variation.

Recently, $\langle g_s \rangle$ has been approximated from sap flux (J_S) measurements scaled to E_L (Köstner et al. 1992, Arneeth et al. 1996, Granier et al. 1996, Martin et al. 1997, Oren et al. 1998, Pataki et al. 1998a, 1998b, Phillips and Oren 1998, Oren et al. 1999a). When leaf and air temperature are similar, a condition that occurs for small leaves exposed to a sufficiently high wind speed (Herbst 1995, Martin et al. 1999), the bulk air vapor pressure deficit (D) can be used as an approximation of δ_w for calculating g_s (Monteith and Unsworth 1990). Under such conditions, calculation of $\langle g_s \rangle$ from sap-flux-scaled E_L (hereafter, G_S) can be simplified as suggested by Monteith and Unsworth (1990):

$$G_S = \frac{K_G(T_A) E_L}{D}, \quad (2)$$

where G_S is mean canopy stomatal conductance to water vapor (m s^{-1}), K_G is the conductance coefficient as a function of temperature ($115.8 \pm 0.4236 \text{ kPa m}^3 \text{ kg}^{-1}$)—accounting for temperature effects on the psychrometric constant, latent heat of vaporization, specific heat of air at constant pressure, and the density of air—and T_A is bulk air temperature ($^{\circ}\text{C}$). Phillips and Oren (1998) showed that errors associated with lumping the temperature-dependent physical coefficients into K_G are negligible.

Because sap-flux-scaled G_S is the product of measurements representing relatively large leaf areas, it is subject to certain

sources of error. These include errors in estimating E_L and δ_w because of systematic and random variations and instrument limitations. This study was designed to generate a conditional sampling scheme aimed at keeping the effect of measurement errors in the estimate of G_S to within 10% of the measurement error-free estimate.

Errors in estimating E_L

Sap-flux-scaled E_L may represent water uptake rather than transpiration if the quantity of water discharged from storage in the plant into the transpiration stream in the morning is large relative to uptake, and the quantity recharged by uptake late in the day is large relative to transpiration (Granier et al. 1996, Phillips et al. 1996, Loustau et al. 1998, Phillips and Oren 1998). To assess if J_S can be used to calculate G_S in this stand, we evaluated the effect of stem water storage capacity on E_L by comparing a time series of stem J_S measured with Granier-type sensors with branch J_S measured with Kučera-type sensors (Cienciala et al. 1994) in the top and bottom branches of the canopy.

Increasingly, sap flux in the hydroactive xylem is estimated with Granier-type sensors (Granier 1987), which measure the maximum temperature difference between heated and unheated probes during times of zero flux (ΔT_M) as a baseline. Temperature difference (ΔT) is also measured during the day as water carries heat away from the probe. Deviation from the baseline is used to estimate water flux. Granier-type sensors may be sensitive to temperature gradients in the stem creating an apparent temperature difference (Goulden and Field 1994, Köstner et al. 1998). This error can be large when fluxes are low, and trees are small (Granier 1987). Additional errors, even in large trees, may be caused by uncertainties in the baseline position (i.e., ΔT_M). Therefore, we quantified the effect of uncertainties in ΔT_M on estimates of diurnal time courses of J_S .

Errors in estimating δ_w

Calculation of D requires measurements of relative humidity of bulk air (R_H), and T_A , and calculations of δ_w require additional measurements of leaf temperature (T_L ; °C). It is often assumed that a single sensor is sufficient to represent D in the canopy (Köstner et al. 1992, Granier et al. 1996, Martin et al. 1997, Oren et al. 1998, Pataki et al. 1998a, 1998b). For well-coupled canopies at sufficiently high wind speeds, D approximates δ_w (Jarvis and McNaughton 1986, Martin et al. 1999), and thus a single R_H-T_A sensor can be used to calculate G_S . In this study, we analyzed the effects of measurement errors on values of δ_w and D and, in turn, on the calculation of G_S . We also tested the assumption that D does not vary horizontally and vertically by performing: (1) concurrent measurements in nearby stands with twofold difference in leaf area index (L) and an adjacent opening, and (2) rapid measurements along a vertical transect within the canopy.

Material and methods

Study site and treatments

The Southeast Tree Research and Education Site (SETRES) was established in 1992 in a stand of *Pinus taeda* L. planted in 1984 in the Sandhills of North Carolina (35° N, 79° W) on an infertile, well-drained, sandy, siliceous, thermic Psammentic Hapludult soil (Wakulla series). Mean annual precipitation is 1210 mm with occasional growing season water deficits. Three treatments were established in addition to a control (C): irrigated (I), fertilized (F), and a combination of irrigation and fertilization (IF). Nutrient treatments have been maintained since March 1992 and irrigation treatments since April 1993. The treatments have resulted in peak L of 1.8, 1.9, 3.3, and 3.6 and basal areas of 14, 14, 20, and 25 m² ha⁻¹ for trees in the C, I, F, and IF treatments, respectively. For details of nutrition and irrigation treatments see Albaugh et al. (1998) and Murthy et al. (1996).

Stem J_S and associated environmental variables were measured from August 1996 to January 1999. During this period, short measurement campaigns were carried out to evaluate potential sources of error.

Sap flux measurements

We measured J_S in stem xylem of eight trees in a 6-m diameter plot and in branch xylem in a subset of three trees within each treatment (Ewers et al. 1999). Measurements on the north side of stems (1.4 m above ground) were made with Granier-type sensors at two depths: the outer 20 mm of the xylem ($J_{S_{out}}$) in eight trees, and, to account for radial patterns in J_S , the next 20 mm of the xylem ($J_{S_{in}}$) in a subset of five trees. The J_S (m³ H₂O m⁻² s⁻¹) is calculated based on the empirical equation (Granier 1987):

$$J_S = 119 \times 10^{-6} \left(\frac{\Delta T_M - \Delta T}{\Delta T} \right)^{1.231} \quad (3)$$

We calculated mean J_S , weighting $J_{S_{out}}$ by the sapwood area represented in that xylem band and $J_{S_{in}}$ by the sapwood area internal to the outer band (Ewers et al. 1999), assuming that $J_{S_{in}}$ represents sap flux in the xylem between 20 and 40 mm from the cambium. On average, sapwood area inside the outer 20-mm band was 15% of the total. On June 12–24, 1998, to evaluate whether scaling must account for a systematic circumferential variance in flux, we installed sensors to measure $J_{S_{out}}$ on the south side of stems of a subset of five trees in C and IF, and compared these with measurements made on the north side. Trees in the C and IF treatments were chosen because they represented the highest and lowest L and differed in sapwood characteristics (Ewers et al. 1999).

We evaluated time lags between water uptake and transpiration by measuring xylem flux with Kučera-type sensors (Cienciala et al. 1994), based on the heat balance method, in upper branches of 6–12 mm diameter and lower branches of 12–18 mm diameter. Branch measurements were made from

July 23 to August 8, 1998. To avoid thermal gradients from direct radiation, all sensors were shielded. Analyses of daily water use were performed on daily sums of J_s from 0500 to 0500 h, corresponding approximately to the time of zero flow, and therefore include nighttime recharge (Phillips and Oren 1998).

To calculate E_L ($\text{kg H}_2\text{O m}^{-2} A_L \text{ s}^{-1}$), J_s ($\text{kg H}_2\text{O m}^{-2} A_s \text{ s}^{-1}$) for either branches or stems is combined with sapwood area ($A_s; \text{m}^2$) and leaf area ($A_L; \text{m}^2$) as follows (Pataki et al. 1998b):

$$E_L = J_s \frac{A_s}{A_L} \quad (4)$$

Environmental measurements

Values of δ_w were calculated from R_H , T_L , and T_A based on equations adapted from Goff and Gratch (1946):

$$V_s = 0.611e^{(17.27T_L)/(T_L + 237)} \quad (5)$$

$$\delta_w = \left(\left(\frac{R_H}{100} \right) V_s \right) - V_s \quad (6)$$

where V_s is saturated water vapor pressure (kPa). Here, δ_w is in kPa and can be converted to mole fractions used in Equation 1 by dividing by atmospheric pressure. The value of D is calculated from Equations 5 and 6, where T_A is substituted for T_L .

During most of the study period, an R_H - T_A probe (Vaisala HMP 35C, Campbell Scientific, Logan, UT) was positioned at the center of each plot at 2/3 distance from the bottom of the canopy (sensor height/stand height, $z/h = 0.79$ - 0.83). During August 2-28, 1997, additional measurements of T_L were made in each treatment by infrared thermometry (Everest Interscience, Palo Alto, CA) based on an emissivity of 0.97 (Gates 1965, Gay and Knoerr, 1975). We used these measurements to test the validity of replacing D with δ_w for calculating G_s . We also used the measurements to assess the effect of horizontal variability in L on D . On July 23 and August 5, 1998, the effect of the vertical distribution of leaf area on the D profile was evaluated by raising and then lowering the sensor 1 m min^{-1} during the midday plateau in the diurnal pattern of D .

Photosynthetic photon flux density (Q) above the canopy was monitored with a quantum sensor (LI-190s, Li-Cor, Lincoln, NE). Xylem flux and all environmental sensors were sampled every 30 s (DL2, Delta-T Devices, Cambridge, U.K.). Thirty-minute mean values were recorded during the study, except for branch J_s for which 15-min averages were recorded.

Structural measurements

At the end of the study, branches monitored for sap flux were harvested. No heartwood was visible in upper or lower branches, but the pith was clearly discernible from the sapwood. Branch sapwood area was determined by subtracting the bark and heartwood areas from the branch cross-sectional area at the midpoint of sensor length. From each branch, five

fascicles were selected randomly from current- and previous-year foliage. The length and width of each needle were measured to ± 1 and ± 0.005 mm, respectively. Projected leaf area was determined by multiplying the width of each needle by its length and then summing the area for the fascicle. Needles were then oven-dried for at least 24 h at 65 °C, weighed, and their specific leaf area ($\text{cm}^2 \text{ g}^{-1}$) determined. The remaining needles of each age class were also oven-dried. Total leaf area of each branch was obtained by multiplying leaf mass in each age class by the respective specific leaf area and summing the area of both age classes.

Heartwood was not present in any stems of any treatments as expected for *P. taeda* of this age (cf. Megraw 1985). Therefore, sapwood area for each tree was calculated from diameter at sensor height. Bark thickness was measured in each tree and differed among treatments (Ewers et al. 1999). After correcting for bark thickness, sapwood area per unit of ground area was calculated by summing the area of all trees in the plot and dividing by plot area. Sapwood area was 9.0, 9.0, 15.2, 21.9 $\text{m}^2 \text{ ha}^{-1}$ for trees in the C, I, F, and IF treatments, respectively (Ewers et al. 1999). Leaf area of each tree was calculated from allometric relationships derived from winter biomass harvests at the site (Albaugh et al. 1998). Leaf area estimates for each tree were corrected for seasonality based on relative increase in leaf area from winter to the sampling period as determined with a leaf area meter (Li-Cor, LAI-2000) and litterfall at the stand level (Ewers et al. 1999). The $A_s:A_L$ ratio was calculated for each tree based on estimates of leaf area and sapwood area. To estimate stand L (projected), "winter equivalent" leaf area of each tree in each subplot was estimated from its diameter and the treatment specific allometric relationships as above (Albaugh et al. 1998, Ewers et al. 1999). Leaf area measurements of all individuals in each subplot were summed, divided by the plot area (133 m^2) and corrected for seasonal leaf area dynamics.

Statistical analyses

All statistical analyses were made with SAS procedures GLM, ARIMA and SPECTRA (Version 6.12, SAS Institute, Cary, NC). Nonlinear curve fits were performed in SIGMAPLOT (Version 4.5, SPSS, San Rafael, CA). Time lags were evaluated by time series analyses performed both in the time and frequency domain according to Brocklebank and Dickey (1986).

Results

Errors in estimates of J_s caused by baseline placement

Occasionally, an apparently stable ΔT_M became unstable in early morning when sap flux began. We chose the most unstable behavior found among all trees as an example in Figure 1. Relatively stable ΔT_M (defined as the portion of ΔT_M that varies within the narrow range of 0.02 mV for at least 2 h) is plotted alongside unstable ΔT_M (defined as the ΔT_M connecting the greatest temperature differences). The maximum difference

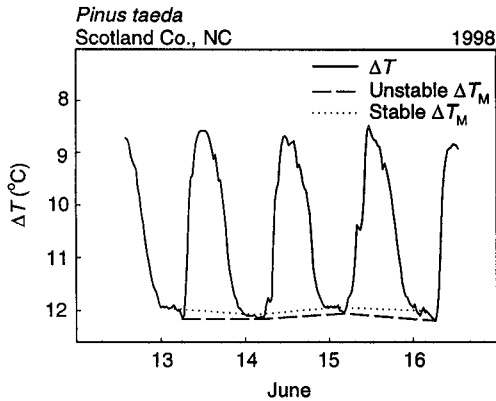


Figure 1. Time series of the temperature difference (ΔT , $^{\circ}\text{C}$) between heated and unheated Granier-type sensors of sap flux (J_S). The solid line is the actual decline in ΔT with increasing sap flux. The dotted line represents the stable maximum temperature difference between the two sensors, which is assumed to occur near zero flux (ΔT_M). The dashed line represents the unstable ΔT_M . See text for definitions of stable and unstable ΔT_M .

between stable and unstable ΔT_M values occurred on June 16 and amounted to 0.1 $^{\circ}\text{C}$, a small fraction of the mean ΔT_M of 12 $^{\circ}\text{C}$.

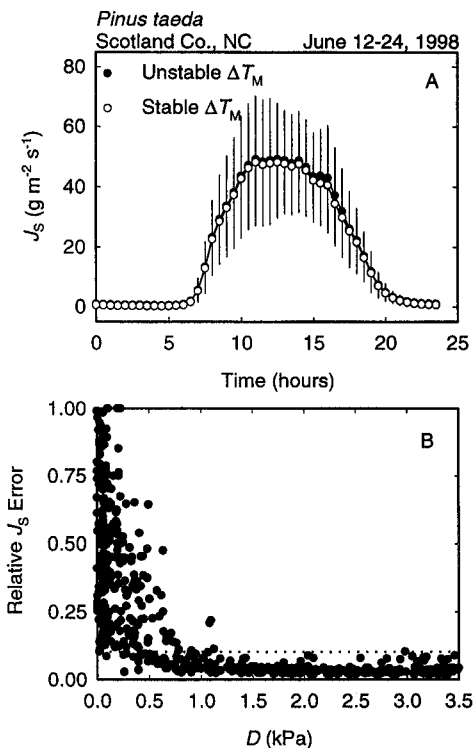


Figure 2. (A) Time-averaged sap flux (J_S) over 12 days based on stable and unstable maximum temperature difference near zero flux (ΔT_M) as shown in Figure 1. The bars are 1 SE over time ($n = 12$). (B) Difference in J_S calculated based on stable and unstable ΔT_M as a fraction of J_S calculated for a stable ΔT_M in relation to vapor pressure deficit (D). The dotted line represents a 10% error.

The effect of the difference between stable and unstable ΔT_M (Figure 1) on the absolute value of J_S was very small (Figure 2A). However, even a small error in ΔT_M placement may cause large errors in estimates of G_S under conditions of low sap flux. The effect of ΔT_M placement on errors in J_S (and thus E_L and G_S) was assessed by normalizing the difference between J_S estimated with stable and unstable ΔT_M by the values obtained with the stable ΔT_M , and relating this relative error in J_S to D (Figure 2B).

Azimuthal and radial patterns in stem J_S

The $J_{S_{\text{out}}}$ in south-facing sensors was a constant proportion of $J_{S_{\text{out}}}$ in north-facing sensors along the entire range of D , but was highly variable at low D (Figure 3). In both the C and IF stands, the ratio of J_S measured toward the south relative to that measured toward the north was unity (paired t -test $P = 0.88$), even after reducing the variability by selecting data corresponding to $D \geq 0.6$ kPa. Therefore, the daily sum of J_S was similar in both directions ($P = 0.86$). Furthermore, the ratio of north to south J_S was similar in both stands ($P = 0.50$).

We quantified the fertilization-induced increases in L and growth rate on the radial change in J_S between the outer 20 mm and the next 20 mm in the xylem. In both the C and IF stands, the $J_{S_{\text{in}}}/J_{S_{\text{out}}}$ ratio was constant with respect to D . However, the daily sums of $J_{S_{\text{in}}}$ and $J_{S_{\text{out}}}$ differed ($P = 0.001$). In the slow-growing C stand, $J_{S_{\text{in}}}$ was 50% of $J_{S_{\text{out}}}$ ($P = 0.008$; Figure 3), whereas $J_{S_{\text{in}}}$ was only 39% of $J_{S_{\text{out}}}$ ($P = 0.003$; Figure 3) in the fast-growing IF stand.

Water uptake versus transpiration

The magnitude of J_S in branches and stems was similar in all treatments. Diurnal patterns of J_S in stems and lower and upper branches of control trees are shown in Figure 4A. Stem J_S val-

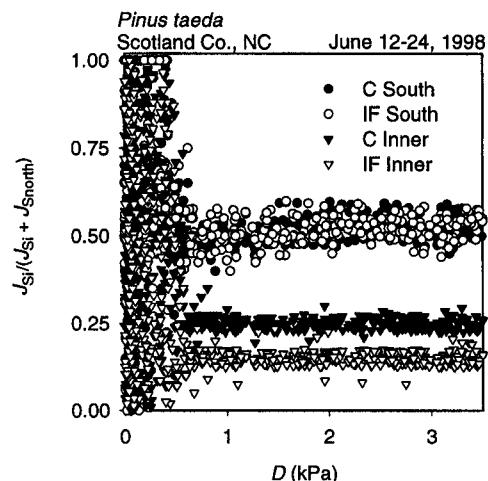


Figure 3. Quotient of sap flux in four positions (J_{S_i} ; where i represents southward, outer or inner sensor) over the sum of J_{S_s} and $J_{S_{\text{north}}}$ in control (C) and irrigated + fertilized (IF) stands in relation to vapor pressure deficit (D).

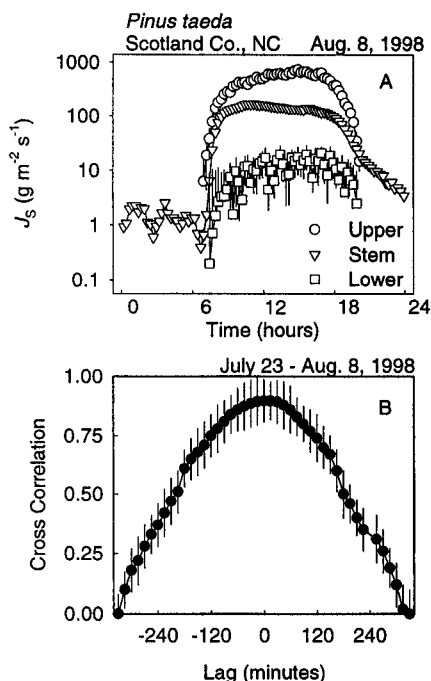


Figure 4. (A) Semi-log plot of diurnal course of sap flux (J_s) in upper and lower branches and stems of trees in the control (C) stand. (B) Cross correlation coefficient between stems and branches in the control stand plotted as a function of lag in minutes. Bars in both (A) and (B) are 1 SEM ($n = 3$).

ues were intermediate between J_s values of the upper and lower branches. Stem J_s continued until 2300 h, whereas J_s of upper and lower branches reached zero flux at 1900 h (effect

Table 1. Autoregression and cross correlation coefficients with vapor pressure deficit (D) in control, irrigated, fertilized, and irrigated + fertilized stands (C, I, F, IF) for the north side and south side of stems and branches in the upper and lower crown. The SEM is one standard error of the mean, $n = 5$ for stem sensors and $n = 3$ for branch sensors. Different letters indicate significant differences at $\alpha = 0.05$ based on least significant differences.

Treatment	Sensor position	Autoregression coefficient (SEM)	Cross correlation coefficient with D (SEM)
C	Stem north	0.64(0.05)a	0.91(0.03)a
C	Stem south	0.62(0.05)a	0.93(0.04)a
I	Stem north	0.63(0.04)a	0.94(0.04)a
F	Stem north	0.79(0.07)b	0.89a(0.06)
IF	Stem north	0.73(0.12)b	0.93(0.03)a
IF	Stem south	0.72(0.15)b	0.90(0.04)a
C	Upper Branch	0.40 (0.08) c	0.76(0.15)a
C	Lower Branch	0.41 (0.11) c	0.87(0.09)a
I	Upper Branch	0.39 (0.11) c	0.85(0.15)a
I	Lower Branch	0.46 (0.07) c	0.79(0.13)a
F	Upper Branch	0.28 (0.05) d	0.86(0.17)a
F	Lower Branch	0.33 (0.05) c	0.85(0.10)a
IF	Upper Branch	0.51 (0.14) ac	0.86(0.12)a
IF	Lower Branch	0.59 (0.09) ac	0.54(0.10)b

masked by log scale in Figure 4A).

The lag between E_L and J_s was analyzed by time series analysis of J_s measured in stems and branches. The dependence of J_s at one time point on the previous point (autoregressive coefficient) was lower in branches than in stems (Table 1) indicating greater variability between consecutive measurements because there is less buffering by stored water in branches than in stems. In addition, J_s of all branches and stems was correlated to D without a lag (Table 1), whereas J_s lagged two hours behind Q . In all cases, the cross-correlation between stem sensors and D was uniformly high (Table 1). Because neither branch nor stem J_s showed a lag with D , branch J_s did not lag stem J_s in any treatment (Figure 4B).

Effect of errors in measurements of R_H and T_A

Measurement errors in T_A were small relative to measurement errors in R_H (Figure 5A). According to the manufacturer's specifications, measurement errors in R_H are $\pm 2\%$ below 90% R_H and $\pm 3\%$ above 90% R_H . The combined effect of measurement errors in R_H and T_A is shown in Figure 5B. Errors in measurement of R_H at 1300 h on June 13 caused an error in D of 5.9%, corresponding to 0.19 kPa. A 0.7 °C error in temperature measurements caused an error of 3.9%.

The time-averaged mean of half-hourly D over a 6-day period, calculated based on a $\pm 2\%$ measurement error below 90% R_H and $\pm 3\%$ above 90% RH, showed a fairly constant absolute difference (Figure 6A). Because the large errors in R_H measurement during periods of high R_H would have caused R_H to be greater than 100% especially at nighttime, we set these

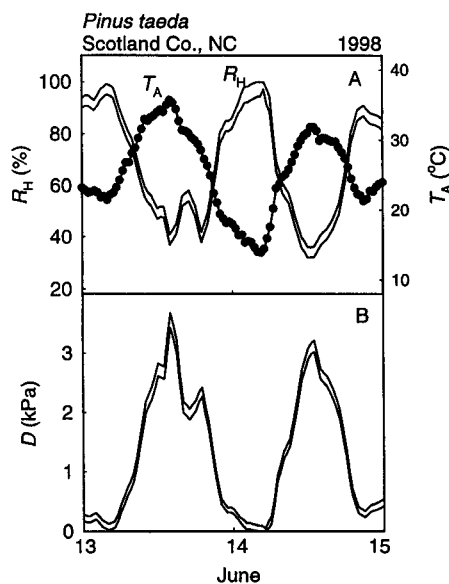


Figure 5. (A) Relative humidity (R_H) shown as two solid lines representing the highest and lowest R_H associated with measurement error. Measurement errors in bulk air temperature (T_A) were too small to be discerned. (B) Vapor pressure deficit (D) calculated from the R_H and T_A values in Panel A. The two lines represent the highest and lowest D values resulting from measurement error.

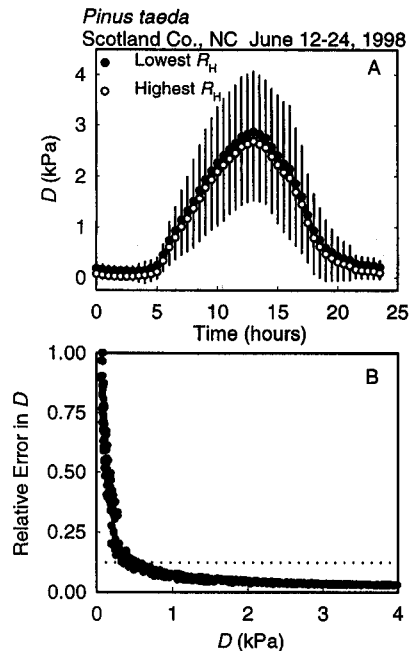


Figure 6. (A) Time-averaged vapor pressure deficit (D) over 12 days calculated using the mean relative humidity \pm measurement error shown in Figure 5A. Bars represent 1 SEM across all days ($n = 12$). (B) The difference between the two D estimates at each measurement as a fraction of the lower estimate in relation to D .

R_H values to 100%. Similarly, the highest value of the lower estimate of R_H cannot exceed 97%. These limits predictably affected the error analysis at high R_H values. Even when using the actual data (without generating a time average), the error increased to above 10% at $D < 0.6$ kPa (Figure 6B), a D value that is typically exceeded for 12 h on a sunny day at this site.

Vertical gradients of R_H , T_A , and D

We evaluated the assumption that there is a negligible vertical gradient in R_H and T_A in well-coupled stands representing a twofold difference in L under conditions of both dry soil surface and during a period of continuous irrigation. The measurements were contrasted with those taken in a nearby opening. There was no vertical gradient in R_H with depth in the canopy regardless of L and the values of all stands were similar to the value found in the opening (Figure 7A). The effect of irrigation was noticeable only lower in the profile where it directly impacted the sensor at 2.8 m (Figure 7B). The vertical profile of T_A generally showed similar responses to those of R_H except that T_A was 1 °C lower during the cooler, unirrigated day than in the opening and 2 °C lower during the warmer, irrigated day (Figures 7C and 7D). The high T_A near the soil surface of the fertilized stands may reflect their location near a large opening that may have provided heat through advection to the space between the soil surface and the base of the canopy at 2 m in the two high- L plots.

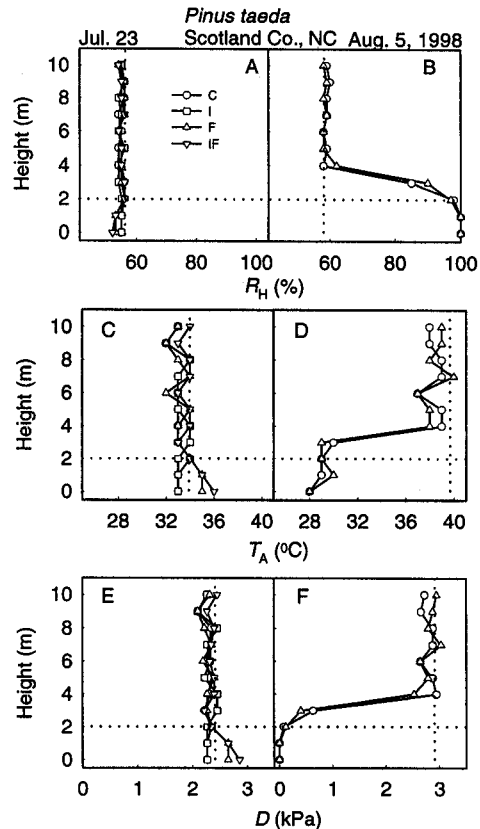


Figure 7. Vertical profiles of relative humidity (R_H), bulk air temperature (T_A) and vapor pressure deficit (D) in control, irrigated, fertilized, and irrigated + fertilized (C, I, F, IF, respectively) plots. Values in (A), (C), and (E) were obtained when irrigation was not applied. Values in (B), (D), and (F) were obtained in plots C and F during a time of a continuous irrigation to a height of 2.8 m. Vertical lines represent the corresponding value taken from a sensor located in a nearby clearing. Horizontal lines represent the mean height of the lowest foliage.

Difference between D and δ_w

There was a linear relationship between T_L and T_A ($P = 0.002$, $R^2 = 0.99$) with a slope of unity and an intercept of 0.03 °C ($P = 0.01$, Figure 8A). The difference between T_L and T_A reached a maximum of 0.1 °C at 12 °C $> T_A > 33$ °C. In early morning, dew formation on the T_A sensor probably depressed its temperature below the true T_A , and during midday hours of high radiation load T_L was probably slightly greater than T_A .

The relationship between D and δ_w was close to unity regardless of whether the measurement error in R_H was considered (Figure 8B). The largest difference observed between δ_w and D was 0.27 kPa at $\delta_w = 4.42$ kPa, a difference of 6%.

Diurnal distribution of errors in G_s

Diurnal patterns of J_s in stems and branches of the C stand during one clear day and one cloudy day with early morning showers were converted to G_s estimates (Figure 9). The random variability among individuals is shown as SE either in as-

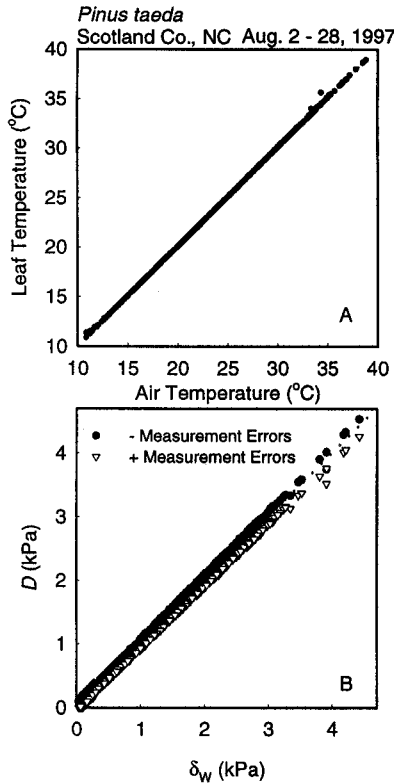


Figure 8. (A) Leaf temperature (T_L) plotted as a function of air temperature (T_A). (B) Vapor pressure deficit (D) plotted as a function of leaf-to-air vapor pressure deficit (δ_w). The uncertainty caused by errors in relative humidity measurements was incorporated into both the D and δ_w estimates.

sociation with the means of J_S (Figures 9A and 9B), or for clarity above the means of G_S (Figures 9C–H). Variability was higher among branches ($n = 3$) than among stems ($n = 8$) and was highest in the upper branches (Figure 9C–F) owing to the asynchronous high frequency fluctuation in branch J_S during the day. The effect of using high and low estimates of D (i.e., reflecting low and high estimates of R_H) is shown by the difference between the lines representing low and high G_S , respectively (Figure 9C–H). The difference between the low and high estimates of D contributed most to the difference in estimates of G_S in the early morning and late afternoon of the clear day. For G_S estimated from stem J_S , additional large errors were introduced by baseline uncertainties (Figures 9G and 9H). The errors were particularly large in the early morning and evening hours when the combined effect of measurement errors in J_S and D produced estimates of G_S that ranged from 0 to 100 $\text{mmol m}^{-2} \text{s}^{-1}$. During the night before the cloudy day, a stable baseline was not attained (Figure 9H). Although the uncertainty in G_S caused by the unstable baseline began to decrease with increasing J_S in the morning, R_H and its associated errors increased in mid-morning because of rains, causing the uncertainty in estimates of G_S to remain high until noon. In addition to errors in estimating G_S caused by measurement errors

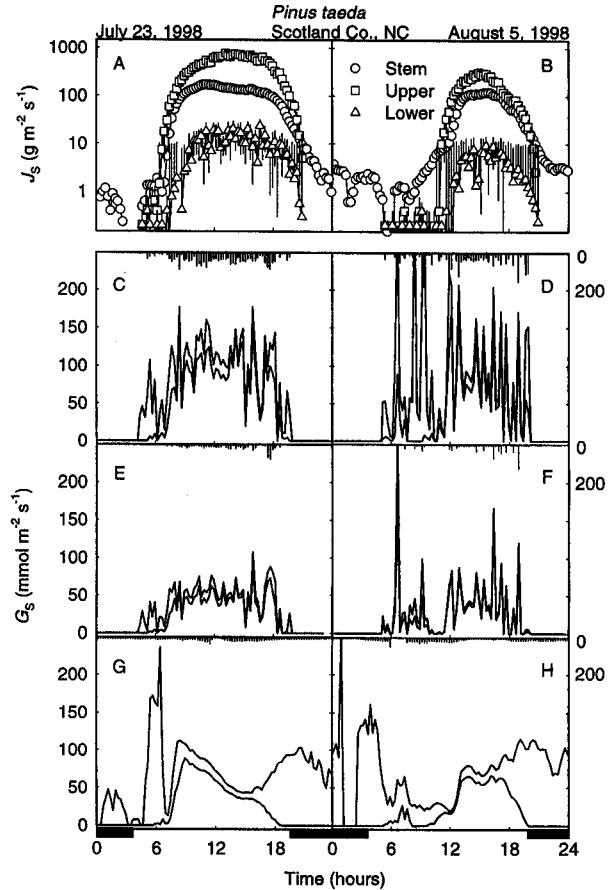


Figure 9. Semi-log plot of diurnal courses of sap flux (J_S) measured with Granier-type sensors in stems, and Kučera-type sensors in top and bottom branches in the control stand during a clear day (A) and a rainy day (B). Bars are 1 SEM ($n = 3$). Diurnal courses of sap-flux-scaled canopy stomatal conductance (G_S) for the same days as in (A) and (B) are shown for upper branches in (C) and (D), lower branches in (E) and (F), and for the stems in (G) and (H). The two lines each represent high and low estimations of G_S incorporating measurement errors that affect vapor pressure deficit (D) in branches and both D and J_S in stems. The descending bars are 1 SEM ($n = 3$), and the scale is shown on the right-side y-axis. Nighttime hours are shown at the bottom.

in J_S and D , stem recharge with water during the night produced artificial nighttime G_S values (Figures 9G and 9H).

Errors in G_S calculated from measurements of J_S in branches decreased to less than 10% at $D \geq 0.6$ kPa, whereas errors in G_S calculated from measurements of J_S in stems decreased to the same value at $D \geq 1.0$ kPa (Figure 10A). Measurement errors in Kučera-type sensors were not assessed, and the difference in D above which similar errors in G_S are produced by both sensors may change if this error is included.

Discussion

We evaluated the effects of measurement errors in J_S , R_H , and T_A on estimates of E_L and δ_w . We also evaluated the impact of

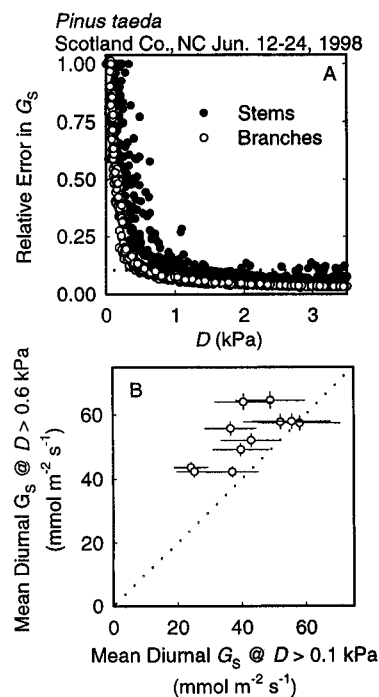


Figure 10. (A) Difference between the high and low estimates of sap flux-scaled canopy stomatal conductance (G_s), shown in Figure 9, as a fraction of the lower estimate in relation to vapor pressure deficit (D). Error in G_s estimates based on stem J_s include errors in J_s and D , whereas those based on branch J_s include only errors in D . (B) Mean diurnal G_s calculated using values of $D \geq 0.1$ kPa (after Phillips and Oren 1998), in relation to mean diurnal G_s calculated using values of $D \geq 0.6$ kPa.

spatial variation in J_s (both radially and azimuthally) on E_L , and the assumption that D at one position in the canopy can be used as a surrogate for δ_w to calculate G_s . All of these errors, systematic variations, and assumptions are inherent to many recent studies in which sap flux is used to estimate G_s (Köstner et al. 1992, Granier et al. 1996, Martin et al. 1997, Pataki et al. 1998a, 1998b, Oren et al. 1999a).

Estimating E_L from sap flux measurements

Use of sap flux measurements to estimate E_L is problematic because of the potential effects of baseline error in J_s measurements, systematic spatial variation in J_s , and a lag between water uptake and transpiration caused by water storage in the stem. Typically, a stable ΔT_M is realized sometime at night, and is reached at a later hour as soil dries (Phillips et al. 1996). Goulden and Field (1994) used a small ΔT_M value (2.2 °C) and found that temperature gradients in the afternoon can cause relatively large ΔT_M shifts in trees of similar size. In this study, ΔT_M was large (12 °C, Figure 1) and thermal gradients never exceeded 0.01 °C (Ewers et al. 1999), thus making our setup less sensitive to thermal gradient. The error in J_s caused by uncertainties in ΔT_M can be high at low D , corresponding to early

morning, late afternoon, and nighttime (Figure 2B). The relative error in J_s was less than 10% at $D \geq 0.6$ kPa and stabilized at approximately 4% at $D \geq 1$ kPa.

Scaling of sap flux in small xylem patches to the entire stem is based on quantifying circumferential and radial patterns in xylem sap flux (Granier et al. 1996, Phillips et al. 1996, Čermák and Nadezhdina 1998, Oren et al. 1998). In *Taxodium distichum* (L.) L. Rich., sap flux on the north side of trees was 64% of that in directions 120° from the north (Oren et al. 1999b). We found no difference in J_s between the north and south sides of trees (Figure 3). Although fertilization increased L from 1.8 to 3.6, the resulting light and radiation differences did not produce azimuthal changes in J_s , perhaps reflecting low variation among measurements made near the base of crowns (Loustau et al. 1998).

Inner, juvenile xylem in *P. taeda* stands of similar age and moderate growth rate showed a 45% decline in J_s relative to the outer, mature wood (Phillips et al. 1996). The radial decrease in J_s was 50% in the slow-growing C stand and 39% in the fast-growing IF stand (Figure 3), reflecting changes in wood properties and growth rate in response to fertilization (Ewers et al. 1999). It appears that J_s decreases with depth more in fast-growing trees than in slow-growing trees. We conclude that measurements in the outer xylem alone should not be used in comparative studies among individuals and stands growing at different rates, especially when the sapwood includes juvenile wood.

Calculating G_s from J_s requires corrections for the lag between water uptake and transpiration (Schulze et al. 1985, Granier et al. 1996, Martin et al. 1997). Commonly, the lag is estimated from a formal or informal time series analysis of environmental variables and J_s (Diawara et al. 1991, Granier and Loustau 1994, Phillips et al. 1997). Time lags between J_s in stems and environmental variables range from 0 to 3.5 h and are not clearly related to tree size or measurement distance below the crown (Schulze et al. 1985, Köstner et al. 1992, Granier et al. 1996, Loustau et al. 1996, Martin et al. 1997, Phillips et al. 1997). Alternatively, one can measure J_s simultaneously in branches and in the stem and estimate the lag between the resulting time series (Meinzer et al. 1997). The use of J_s in branches is justified when the branches are considered to represent the entire crown and store negligible amounts of water.

Sap flux in branches began about the same time as sap flux in the stem, but ceased earlier in the evening as transpiration stopped; whereas water uptake for stem recharge continued (Figures 4A and 9A). Time series analysis indicated that water storage in branches is much less than in the stem (Table 1). However, both time and frequency domain analyses indicated that J_s in stems did not lag either J_s in branches or D (Figure 4B, Table 1). Although this justifies using J_s in stems and branches to calculate G_s without lag, the observed nighttime uptake in stems (Figures 4A and 9A) indicates that G_s calculated from J_s in stems may be underestimated early in the morning and overestimated late in the afternoon. Phillips and Oren (1998) proposed a conditional sampling approach designed to select times when these errors are small.

Estimating δ_w

Estimates of G_S suffer not only from errors in estimating J_S (Figure 2B) and stem recharge (Figures 4A and 9A) but also from errors in estimating the driving force for transpiration. Errors in the driving force may originate from measurement errors of T_L , T_A , and R_H , and from systematic variation along the canopy profile. Castellvi et al. (1996) found that R_H estimated from mean daily dewpoint temperature, mean daily T_A , and diurnal pattern of T_A had an error of up to 9% compared with R_H measured with the more accurate but less automated dewpoint hygrometer. Given patterns in T_A and R_H found in this study (Figure 5A), the largest measurement errors in T_A translated to a maximum error in D of 3.9%. However, errors in measurement of R_H may cause large errors in D , exceeding 10% when $D < 0.6$ kPa (Figures 5B, 6A and 6B).

In well-coupled stands when wind speed is sufficiently high (Martin et al. 1999), T_L is often assumed to be similar to T_A , justifying the use of D as a proxy for δ_w for calculating G_S (Köstner et al. 1992, Granier et al. 1996, Martin et al. 1997, Oren et al. 1998). We did not evaluate the effect of errors in estimates of emissivity on the measurement of T_L with an infrared thermometer, but these errors can be large (Gay and Knoerr 1975). Provided that the emissivity used in this study is correct, T_L was indistinguishable from T_A (Figure 8A) justifying the use of D as a surrogate for δ_w (Figure 8B).

In most studies, D is calculated for one position within or above the canopy (Köstner et al. 1992, Granier et al. 1996, Martin et al. 1997, Oren et al. 1998, Pataki et al. 1998a, 1998b). This assumes that vertical gradients in T_A and R_H are small and their effects on G_S estimates are negligible. Temperature gradients may be as high as 5 °C in shrub canopies and 17 °C in pasture (Tappeiner and Cernusca 1996), both of which are less aerodynamically turbulent than many coniferous and some broadleaf forests. In coniferous and other forests with high canopy roughness, the air within the canopy is considered well mixed with the air above the canopy, at least during daytime when the mechanical production of turbulent kinetic energy is high (Oke 1995). This should result in a relatively weak gradient of D within the canopy.

In forests where aerodynamic turbulence is low, the simplification of Equation 2 cannot be used and a radiative term must be added (Monteith and Unsworth 1990). Furthermore, multiple measurements of D would be needed in a vertical array to measure the vertical gradients of D that result in forests of low aerodynamic conductance. Aerodynamic conductance in all stands at our study site was estimated to be 33-fold higher than total canopy conductance (Ewers et al. 1999). This difference is reflected in the similarity observed between D in an opening and D inside stands differing twofold in L and the absence of a vertical gradient in D (Figure 7). This is similar to findings in a *Pinus sylvestris* L. stand ($L = 2.8$, height = 12 m), where D changed vertically only at an aerodynamic conductance of 0.001 kPa m⁻¹ (Joss and Graber 1996). At our study site, a gradient in D below the canopy was found only under conditions caused by irrigation or a nearby large opening (Figures 7E and 7F). Thus, the assumption that a single R_H - T_A sensor is

sufficient to provide an estimate of D throughout the canopy is valid for *P. taeda* and similar forests.

Conditional sampling approaches for calculating G_S

Analysis of measurement errors indicated that, to estimate G_S within 10% of error-free values, data should be selected for $D \geq 0.6$ to 1.0 kPa (Figure 10A). Phillips and Oren (1998) employed a statistically based conditional sampling approach to reduce the errors in estimating G_S . This statistical approach removed from the analysis rain days, all values of G_S corresponding to times in which $D < 0.1$ kPa, and all days with less than 12 G_S values after applying the second criterion. Based on these selection criteria, an acceptable agreement was obtained between the mean of the remaining half-hour data and a mean daily G_S ($\langle G_S \rangle$) computed directly from the daily sum of J_S and the daily mean daytime D . Phillips and Oren (1998) anticipated that the mean of diurnal G_S values will be lower than $\langle G_S \rangle$ because, unlike $\langle G_S \rangle$, G_S does not incorporate the water that is transpired during the day but taken up during the night. Based on the criteria for conditional sampling obtained here (i.e., $D \geq 0.6$ kPa), mean diurnal G_S values were generally greater than $\langle G_S \rangle$, and there was no difference between use of $D \geq 0.6$ kPa or $D \geq 1.0$ kPa as a filter ($P > 0.5$). As a result, the G_S calculated as recommended here was higher than that calculated as suggested by Phillips and Oren (1998; Figure 10B); however, the means estimated by two approaches converged for days of high conductance.

The conditional sampling method proposed here does not exclude rain days and is not limited by a requisite minimum number of points for estimating G_S , unlike the statistically based approach proposed in Phillips and Oren (1998). However, the statistically based approach permits use of data when D is low (i.e., $D \geq 0.1$ kPa). Environmental conditions may dictate which approach is used to calculate G_S (e.g., the statistically based approach may be more suitable in moist environments where a large proportion of the data would be excluded at $D < 0.6$ kPa). Nevertheless, the approach developed here limits the data to the range in which estimates of G_S have a lower uncertainty (Figure 10A).

Acknowledgments

This research was funded by USDA Forest Service Grant and Westvaco Co., the National Science Foundation through Grant BIR-9512333, and the US Department of Energy through the Southeast Regional Center at the University of Alabama (Cooperative Agreement No. DE-FC03-90ER61010). The authors are grateful to Peter Anderson and Greg Burkland for technical assistance. This work contributes to the Global Change and Terrestrial Ecosystem (GCTE) core project of the International Geosphere-Biosphere Program (IGBP).

References

- Albaugh, T.J., H.L. Allen, P.M. Dougherty, L.W. Kress and J.S. King. 1998. Leaf area and above- and belowground growth responses of loblolly pine to nutrient and water additions. *For. Sci.* 44:317–328.

- Arneth, A., F.M. Kelliher, G. Bauer, D.Y. Hollinger, J.N. Byers, J.E. Hunt, T.M. McSeveny, W. Ziegler, N.N. Vygodskaya, I. Milukova, A. Sogachov, A. Varlagin and E.-D. Schulze. 1996. Environmental regulation of xylem sap flow and total conductance of *Larix gmelinii* trees in eastern Siberia. *Tree Physiol.* 16:247–255.
- Baldocchi, D. and T. Meyers. 1998. On using eco-physiological, micrometeorological and biogeochemical theory to evaluate carbon dioxide, water vapor and trace gas fluxes over vegetation: a perspective. *Agric. For. Meteorol.* 90:1–15.
- Brocklebank, J.C. and D.A. Dickey. 1986. SAS system for forecasting time series. SAS Institute Inc., Cary, NC, 240 p.
- Castellvi, F., P.J. Perez, J.M. Villar and J.I. Rosell. 1996. Analysis of methods for estimating vapor pressure deficits and relative humidity. *Agric. For. Meteorol.* 82:29–45.
- Cienciala, E., A. Lindroth, J. Čermák, J.-E. Hallgren and J. Kučera. 1994. The effects of water availability on transpiration, water potential and growth of *Picea abies* during a growing season. *Trees* 6:121–127.
- Čermák, J. and N. Nadezhdina. 1998. Sapwood as the scaling parameter—defining according to xylem water content or radial pattern of sap flow. *Ann. Sci. For.* 55: 409–521.
- Diawara, A., D. Loustau and P. Berbigier. 1991. Comparison of two methods for estimating the evaporation of a *Pinus pinaster* (Ait.) stand: sap flow and energy balance with sensible heat flux measurements by an eddy covariance method. *Agric. For. Meteorol.* 54:49–66.
- Ewers, B.E., R. Oren, T.J. Albaugh and P.M. Dougherty. 1999. Carry-over effects of long term water and nutrient supply on short term water use in *Pinus taeda* trees and stands. *Ecol. Appl.* 9:513–525.
- Gates, D.M. 1965. Radiant energy, its receipt and disposal. *Meteorol. Monogr.* 6:1–26.
- Gay, L.W. and K.R. Knoerr. 1975. The forest radiation budget. Duke University School of Forestry and Environmental Studies. Durham, NC, 165 p.
- Goff, J.A. and S. Gratch. 1946. List 1947, Smithsonian Meteorological Tables. *Trans. Am. Soc. Ventilation Engineer.* 52:95.
- Goulden, M.L. and C.B. Field. 1994. Three methods for monitoring the gas exchange of individual tree canopies: ventilated-chamber, sap-flow and Penman-Monteith measurements on evergreen oaks. *Funct. Ecol.* 8:125–135.
- Granier, A. 1987. Evaluation of transpiration in a Douglas-fir stand by means of sap flow measurements. *Tree Physiol.* 3:309–320.
- Granier, A. and D. Loustau. 1994. Measuring and modeling the transpiration of a maritime pine canopy from sap-flow data. *Agric. For. Meteorol.* 71:61–81.
- Granier, A., P. Biron, B. Köstner, L.W. Gay and G. Najjar. 1996. Comparisons of xylem sap flow and water vapour flux at the stand level and derivation of canopy conductance for Scots pine. *Theor. Appl. Climat.* 53:115–122.
- Herbst, M. 1995. Stomatal behavior in a beech canopy: an analysis of Bowen ratio measurements compared with porometer data. *Plant Cell Environ.* 18:1010–1018.
- Hinckley, T.M., D.G. Sprugel, J.R. Brooks, K.J. Brown, T.A. Martin, D.A. Roberts, W. Schaap and D. Wang. 1998. Scaling and integration in trees. *In Ecological Scale: Theory and Application*. Eds. D.L. Peterson and V.T. Parker. Columbia University Press, New York, pp 309–337.
- Jarvis, P.G. 1995. Scaling processes and problems. *Plant Cell Environ.* 18:1079–1089.
- Jarvis, P.G. and K.G. McNaughton. 1986. Stomatal control of transpiration: scaling up from leaf to region. *Adv. Ecol. Res.* 15:1–49.
- Joss, U. and W.K. Graber. 1996. Profiles and simulated exchange of H₂O, O₃, NO₂ between the atmosphere and the HartX Scots pine plantation. *Theor. Appl. Clim.* 53:157–172.
- Köstner, B.M., E.-D. Schulze, F.M. Kelliher, D.Y. Hollinger, J.N. Byers, J.E. Hunt, T.M. McSeveny, R. Meserth and P.L. Weir. 1992. Transpiration and canopy conductance in a pristine broad-leaved forest of *Nothofagus*: an analysis of xylem sap flow and eddy correlation measurements. *Oecologia* 91:350–359.
- Köstner, B., A. Granier and J. Čermák. 1998. Sapflow measurements in forest stands: methods and uncertainties. *Ann. Sci. For.* 55: 13–27.
- Loustau, D., P. Berbigier, P. Roumagnac, C. Arruda-Pacheco, J.S. David, M.I. Ferreira, J.S. Pereira and R. Tavares. 1996. Transpiration of a 64-year-old maritime pine stand in Portugal. I. Seasonal course of water flux through maritime pine. *Oecologia* 91: 350–359.
- Loustau, D., J.-C. Domec and B. Alexandre. 1998. Interpreting the variations in xylem sap flux density within the trunk of maritime pine (*Pinus pinaster* Ait.): application of a model for calculating water flows at tree and stand levels. *Ann. Sci. For.* 55:29–46.
- Leverenz, J., J.D. Deans, E.D. Ford, P.G. Jarvis, R. Milne and D. Whitehead. 1982. Systematic spatial variation of stomatal conductance in a Sitka spruce plantation. *J. Appl. Ecol.* 19:835–851.
- Martin, T.A., K.J. Brown, J. Čermák, R. Ceulemans, J. Kučera, F.C. Meinzer, J.S. Rombold, D.G. Sprugel and T.M. Hinckley. 1997. Crown conductance and tree and stand transpiration in a second growth *Abies amabilis* forest. *Can. J. For. Res.* 27:797–808.
- Martin, T.A., T.M. Hinckley, F.C. Meinzer and D.G. Sprugel. 1999. Boundary layer conductance, leaf temperature and transpiration of *Abies amabilis* branches. *Tree Physiol.* 19:435–443.
- Megraw, R.A. 1985. Wood quality factors in loblolly pine. Tappi, Atlanta, GA, 88 p.
- Meinzer, F.C., T.M. Hinckley and R. Ceulemans. 1997. Apparent responses of stomata to transpiration and humidity in a hybrid poplar canopy. *Plant Cell Environ.* 16:429–426.
- Murthy, R., P.M. Dougherty, S.J. Zarnoch and H.L. Allen. 1996. Effects of carbon dioxide, fertilization, and irrigation on photosynthetic capacity of loblolly pine trees. *Tree Physiol.* 16:537–546.
- Monteith, J.L. and M.H. Unsworth. 1990. Principles of environmental physics. Edward Arnold, London, 291 p.
- Oke, T.R. 1995. Boundary layer climates. Routledge, London, 435 p.
- Oren, R., N. Phillips, G. Katul, B.E. Ewers and D.E. Pataki. 1998. Scaling xylem sap flux and soil water balance and calculating variance: a method for partitioning water flux in forests. *Ann. Sci. For.* 55:191–216.
- Oren, R., J.S. Sperry, G.G. Katul, D.E. Pataki, B.E. Ewers, N. Phillips and K.V.R. Schäfer. 1999a. Survey and synthesis of intra- and interspecific variation in stomatal sensitivity to vapour pressure deficit. *Plant Cell Environ.* 22:1515–1526.
- Oren, R., N. Phillips, B.E. Ewers, D.E. Pataki and J.P. Megonigal. 1999b. Responses of sap flux-scaled transpiration to light, vapor pressure deficit, and leaf area reduction in a flooded *Taxodium distichum* L. forest. *Tree Physiol.* 19:337–347.
- Pataki, D.E., R. Oren and D.T. Tissue. 1998a. Elevated carbon dioxide does not affect average canopy stomatal conductance of *Pinus taeda* L. *Oecologia* 117:47–52.
- Pataki, D.E., R. Oren, G. Katul and J. Sigmon. 1998b. Canopy conductance of *Pinus taeda*, *Liquidambar styraciflua* and *Quercus phellos* under varying atmospheric and soil water conditions. *Tree Physiol.* 18:307–315.

- Pearcy, R.W., E.-D. Schulze and R. Zimmerman. 1989. Measurement of transpiration and leaf conductance. *In* Plant Physiological Ecology. Eds. R.W. Pearcy, J. Ehleringer, H.A. Mooney and P.W. Rundel. Chapman and Hall, London, pp 137–160.
- Phillips, N. and R. Oren. 1998. A comparison of daily representations of canopy conductance based on two conditional time-averaging methods and the dependence of daily conductance on environmental factors. *Ann. Sci. For.* 55:191–216.
- Phillips, N., R. Oren and R. Zimmerman. 1996. Radial patterns of xylem sap flow in non-, diffuse-, and ring-porous tree species, *Plant Cell Environ.* 19:983–990.
- Phillips, N., A. Nagchaudhuri, R. Oren and G. Katul. 1997. Time constant for water uptake in loblolly estimated from times series of stem sapflow and evaporative demand. *Trees* 11:412–419.
- Schulze, E.-D., J. Čermák, R. Matussek, M. Penka, R. Zimmerman, F. Vasicek, W. Gries and J. Kučera. 1985. Canopy transpiration and water fluxes in the xylem of the trunk of *Larix* and *Picea* trees—a comparison of xylem flow, porometer and cuvette measurements. *Oecologia* 66:475–483.
- Sellers, P.J, R.E. Dickinson, D.A. Randall, et al. 1997. Modeling the exchange of energy, water, and carbon between continents and the atmosphere. *Science* 275:502–509.
- Tappeiner, U. and A. Cernusca. 1996. Microclimate and fluxes of water vapour, sensible heat and carbon dioxide in structurally differing subalpine plant communities in the central Caucasus. *Plant Cell Environ.* 19:403–417.